Fluorenylidene Bridged Cyclotriphosphazenes: 'Turn-Off' Fluorescence Probe for Cu^{2+} and Fe^{3+}

Gönül Yenilmez Çiftçi,* Elif Şenkuytu, Mahmut Durmuş, Fatma Yuksel and Adem Kılıç

Department of Chemistry, Gebze Institute of Technology, Gebze 41400, Kocaeli, Turkey

yenilmez@gyte.edu.tr

Supporting Information

TABLE OF CONTENTS

Figure S1. (a) ^{1}H NMR spectrum of compound **4** in $CDCl_3$ between 0 – 8.5 ppm. (b) ^{1}H NMR expanded spectra between 7.00-8.00 ppm. 3

Figure S2. (a) ^{1}H NMR spectrum of compound **8** in $CDCl_3$ between 0 – 9.00 ppm. (b) ^{1}H NMR expanded spectra between 4.50-7.80 ppm 4

Table S1. ^{1}H NMR spectral data of compounds **3-6** in $CDCl_3$..... 5

Table S2. ^{1}H NMR spectral data of compounds **8-11** in $CDCl_3$ 6

Table S3. Selected bond lengths (Å), bond angles (°) and torsion angles (°) for compounds **4**, **8** and **9** 7

Figure S3. The selected bond angles of compounds **4**, **8** and **9**..... 9

Figure S4. The angles between the planes of aniline or phenol rings of compounds **4** and **8.**10

Figure S5. The angles between the planes of cyclotriphosphazene and aniline or phenol rings of compounds **4**, and **8** 11

Figure S6. The angles between the planes of cyclotriphosphazene rings of compounds **4**, **8** and **9** 12

Figure S7. The angles between the planes of aniline rings of each FDA bridges of compound **9.**..... 13

Figure S8. The angles between the planes of two fluorenylidene rings of compound **9.**..... 14

Figure S9. (A) Fluorescence response of chemosensor **3** to various equivalents of Cu^{2+}. (B) The Benesi-Hildebrand graph and (C) Job's plot of **3**-Cu^{2+} complex in THF solutions. The total concentration of **3** and Cu^{2+} was $1x10^{-2}$ M. The excitation wavelength was 270 nm. The monitored wavelength was 325 nm. 15

Figure S10. The proposed interaction between chemosensor **3** and Cu^{2+} ions.……..…..15

Figure S11. (A) Fluorescence response of chemosensor **3** to various equivalents of Fe^{3+}. (B) The Benesi-Hildebrand graph and (C) Job's plot of **3**-Fe^{3+} complex in THF solutions. The total concentration of **3** and Fe^{3+} was $1x10^{-3}$ M.. The excitation wavelength was 270 nm. The monitored wavelength was 325 nm.....16

Figure S12. The proposed interaction between chemosensor **3** and Fe^{3+} ions.....16

Figure S13. (A) Fluorescence response of chemosensor **4** to various equivalents of Cu^{2+}. (B) The Benesi-Hildebrand graph and (C) Job's plot of **4**-Cu^{2+} complex in THF solutions. The total concentration of **4** and Cu^{2+} was $1x10^{-2}$ M. The excitation wavelength was 270 nm. The monitored wavelength was 320 nm.....17

Figure S14. The proposed interaction between chemosensor **4** and Cu^{2+} ions.....17

Figure S15. (A) Fluorescence response of chemosensor **4** to various equivalents of Fe^{3+}. (B) The Benesi-Hildebrand graph and (C) Job's plot of **4**- Fe^{3+} complex in THF solutions. The total concentration of **4** and Fe^{3+} was $1x10^{-3}$ M The excitation wavelength was 270 nm. The monitored wavelength was 320 nm.....18

Figure S16. The proposed interaction between chemosensor **4** and Fe^{3+} ions.....18

Figure S17. The proposed interaction between (A) **5** and Cu^{2+} ions and (B) **5** and Fe^{3+} ions.....19

Figure S18. (A) Fluorescence response of chemosensor **6** to various equivalents of Cu^{2+}. (B) The Benesi-Hildebrand graph and (C) Job's plot of **6**-Cu^{2+} complex in THF solutions. The total concentration of **6** and Cu^{2+} was $1x10^{-2}$ M. The excitation wavelength was 270 nm. The monitored wavelength was 314 and 322 nm.....20

Figure S19. The proposed interaction between chemosensor **6** and Cu^{2+} ions.....20

Figure S20. (A) Fluorescence response of chemosensor **6** to various equivalents of Fe^{3+}. (B) The Benesi-Hildebrand graph and (C) Job's plot of **6**- Fe^{3+} complex in THF solutions. The total concentration of **6** and Fe^{3+} was $1x10^{-3}$ M. The excitation wavelength was 270 nm. The monitored wavelength was 314 and 322 nm.....21

Figure S21. The proposed interaction between chemosensor **6** and Fe^{3+} ions.....21

Figure S22. (A) Mass spectrum of compound **10** ESI (*m/z*)$[M+Na]^+$; (B) chloro pattern of compound **10**; (C) computer analyzing of chloro pattern of compound 10.....22

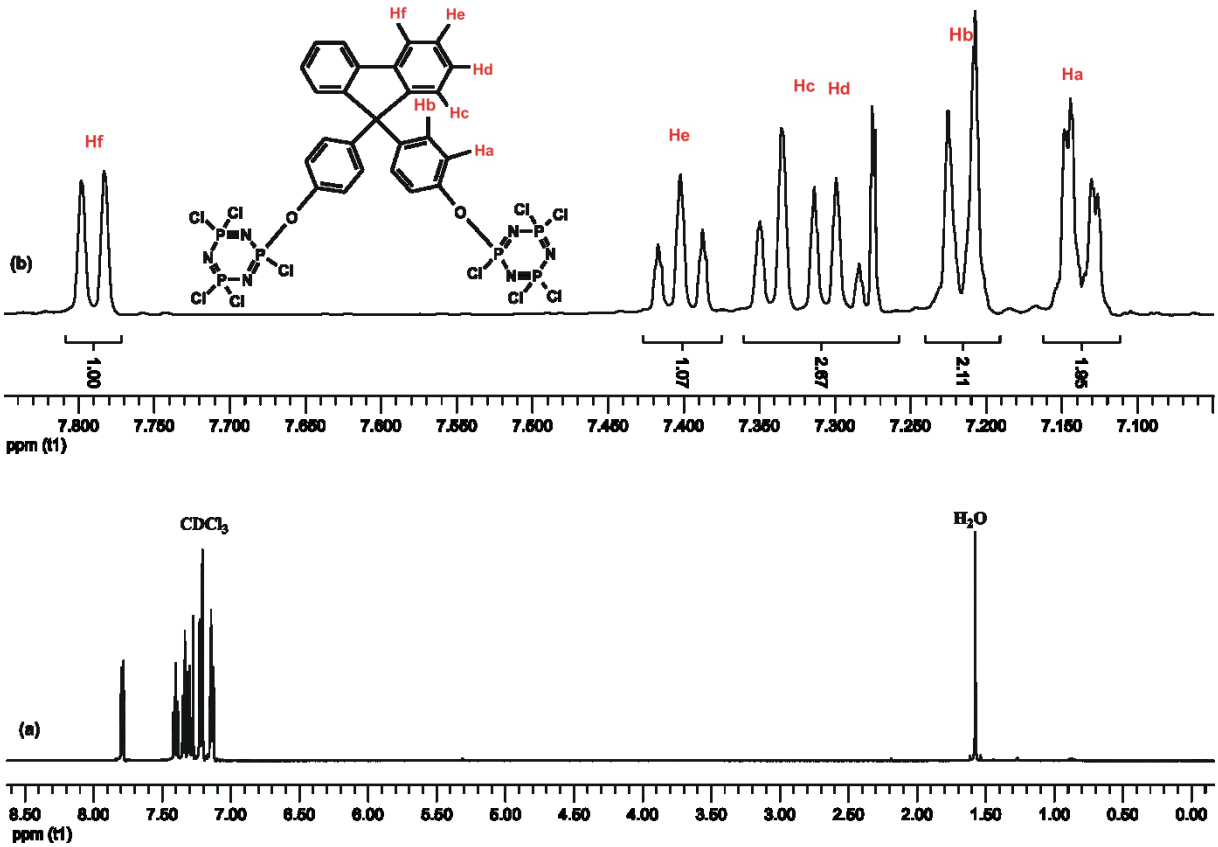

Figure S1. (a) ^{1}H NMR spectrum of compound **4** in $CDCl_3$ between 0 – 8.5 ppm. (b) ^{1}H NMR expanded spectrum between 7.00-8.00 ppm.

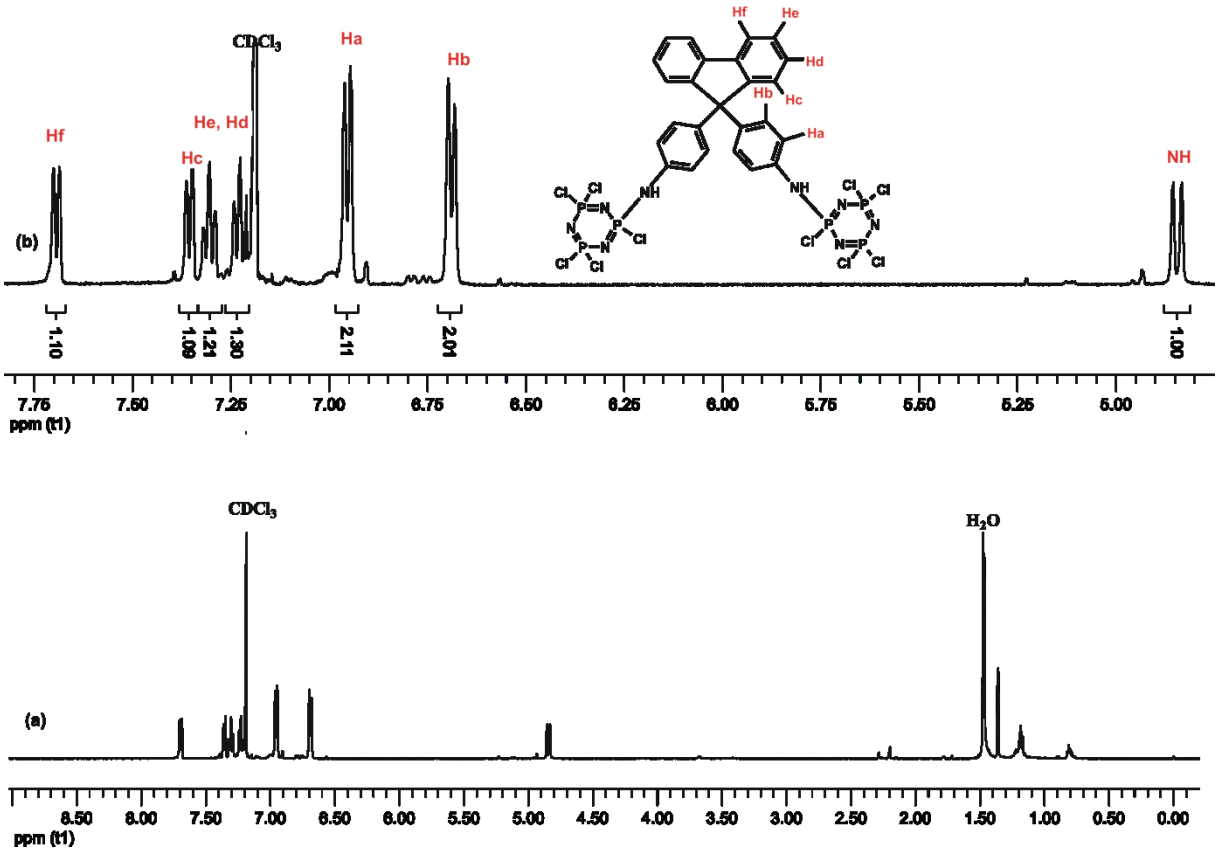

Figure S2. (a) ^{1}H NMR spectra of compound **8** in $CDCl_3$ between 0 – 9.00 ppm. (b) ^{1}H NMR expanded spectra between 4.50-7.80 ppm.

Table S1. ^{1}H NMR spectral data of compounds **3-6** in $CDCl_3$.

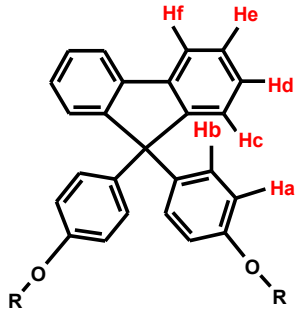

No	Ha	Hb	Hc	Hd	He	Hf	OH
(3)	4H, dd, 6.70, $^{3}J_{HH}$=8.62 $^{4}J_{PH}$=1.28	4H, d, 7.06, $^{3}J_{HH}$=8.61	2H, d, 7.13	2H,m, 7.41-7.23	2H,m, 7.41-7.23	2H, d, 7.84 $^{3}J_{HH}$=7.53	1H, s 5.25
(4)	4H, dd, 7.05 $^{3}J_{HH}$=8.85 $^{4}J_{PH}$=2.04	4H, d, 7.12 $^{3}J_{HH}$=8.84	2H, m 7.27-7.18	2H,m, 7.27-7.18	2H, d, 7.31 $^{3}J_{HH}$=7.36	2H, d, 7.70 $^{3}J_{HH}$=7.50	-
(5)	8H, m, 7.08-7.00	8H, m, 7.21-7.10	4H, m 7.41-7.23	4H,m, 7.41-7.23	4H, m, 7.41-7.23	4H,m, 7.80-7.73	-
(6)	12H, m, 6.96-6.92	12H, m, 7.07-7.01	6H, m 7.32-7.09	6H,m, 7.32-7.09	6H, m, 7.32-7.09	6H,m, 7.64-7.10	-

(**δ** are reported in ppm; **J** values in Hz; **s**, singlet; **d**, doublet; **dd**, doublet of doublet; **m**, multiplet.)

Table S2. ^{1}H NMR spectral data of compounds **8-11** in $CDCl_3$.

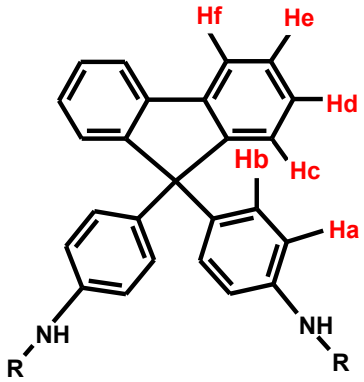

No	Ha	Hb	Hc	Hd	He	Hf	NH
(8)	4H, dd, 6.95, $^{3}J_{HH}$=7.88 $^{4}J_{NHH}$=1.46	4H, d, 6.89, $^{3}J_{HH}$=7.91	2H, d, 7.35 $^{3}J_{HH}$=7.50	2H,t, 7.33-7.21	2H,t, 7.33-7.21	2H,d, 7.69 $^{3}J_{HH}$=7.51	2H, dd, 4.84, $^{2}J_{PH}$=10.93 $^{4}J_{NHH}$=1.60
(9)	8H, d, 7.03 $^{3}J_{HH}$=7.80	8H, d, 6.76 $^{3}J_{HH}$=7.91	4H, d 7.43 $^{3}J_{HH}$=7.46	4H,t, 7.41-7.28	4H,t, 7.41-7.28	4H,d, 7.77 $^{3}J_{HH}$=7.56	4H, d, 4.92 $^{2}J_{PH}$=11.07
(10)	8H, d, 7.14-7.00	8H, d, 6.97-6.78	4H, d, 7.23-7.19	4H,m, 7.41-7.31	4H, m, 7.41-7.31	4H,d, 7.78-7.72	4H, 5.10-5.48
(11)	12H, d, 7.00-6.92	12H, d, 6.82-6.78	6H, m 7.21-7.08	6H,m 7.33-7.13	6H, m, 7.33-7.13	6H,m, 7.73-7.70	6H, 5. 20-5.46

(δ are reported in ppm; **J** values in Hz; **d**, doublet; **dd**, doublet of doublet; **t**, triplet; **m**, multiplet.)

Table S3. Selected bond lengths (Å), bond angles (°) and torsion angles (°) for compounds **4**, **8** and **9**.

	4	**8**	**9**
P1-N1	1.5864(14)	1.593(2)	1.604(3)
P1-N3	1.5750(15)	1.593(2)	1.600(3)
P2-N1	1.5735(16)	1.568(2)	1.562(2)
P2-N2	1.5737(16)	1.584(2)	1.586(3)
P3-N2	1.5823(14)	1.580(2)	1.581(3)
P3-N3	1.5731(15)	1.573(2)	1.563(2)
P4-N4	1.5901(14)		1.594(3)
P4-N6	1.5826(14)		1.605(2)
P5-N4	1.5811(13)		
P5-N5	1.5819(15)		1.588(3)
P6-N5	1.5865(15)		1.593(3)
P6-N6	1.5781(13)		
P1-O1	1.5720(12)		
P4-O2	1.5853(11)		
P1-N7(P1-N4 for 8)		1.622(2)	1.637(3)
P1-N8			1.655(3)
P4-N9			1.639(3)
P4-N10			1.637(3)
O1-C1	1.4075(19)		
O2-C23	1.4239(18)		
N7-C1(N4-C1 for8)		1.423(3)	1.422(4)
N8-C26			1.421(4)
N9-C23			1.427(4)
N10-C48			1.416(4)
N1-P1-N3	117.55(8)	116.85(11)	115.61(13)
N1-P2-N2	118.84(8)	118.07(11)	119.44(14)
N2-P3-N3	118.43(8)	119.51(10)	119.62(14)
N4-P4-N6	117.05(7)		115.42(13)
N4-P5-N5	118.81(8)		
N5-P6-N6	118.31(7)		
P1-N1-P2	121.45(10)	119.83(12)	120.93(16)
P2-N2-P3	120.34(9)	119.45(13)	119.47(16)
P3-N3-P1	122.15(9)	120.23(13)	120.40(16)
P4-N4-P5	122.01(9)		
P5-N5-P6	120.27(9)		119.24(15)
P6-N6-P4	121.88(9)		
C4-C7-C20 (C4-C7-C4# for8)	112.84(12)	111.0(2)	111.0(2)
C29-C32-C45			110.3(2)
P1-O1- C1	126.62(10)		
P4-O2- C23	114.87(9)		
P1-N4- C1		125.01(16)	
P1-N7-C1			123.1(2)
P1-N8-C26			121.7(2)
P4-N9-C23			121.8(2)
P4-N10-C48			124.6(2)
P1-O1-C1-C2	-136.26(13)		

P1-O1-C1-C6	47.5(2)		
P4-O2-C23-C22	-81.44(17)		
P4-O2-C23-C24	97.18(15)		
P1-N4-C1-C2		151.6(2)	
P1-N4-C1-C6		-28.8(3)	
P1-N7-C1-C2			39.5(4)
P1-N7-C1-C6			-139.2(2)
P1-N8-C26-C27			57.2(4)
P1-N8-C26-C31			-122.5(3)
P4-N9-C23-C22			-110.7(3)
P4-N9-C23-C24			68.6(4)
P4-N10-C48-C49			-132.6(3)
P4-N10-C48-C47			46.5(4)

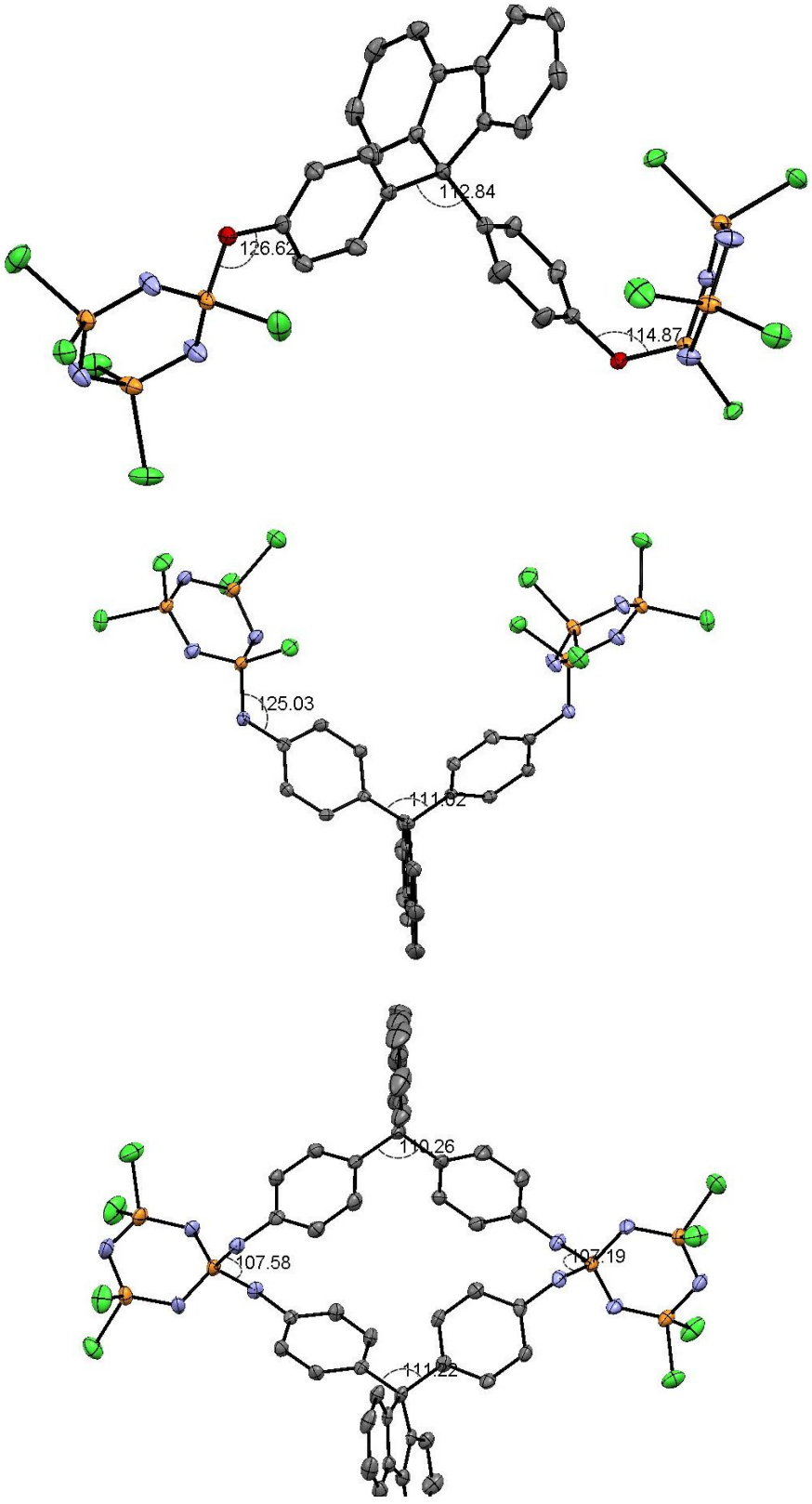

Figure S3. The selected bond angles of compounds **4**, **8** and **9.**

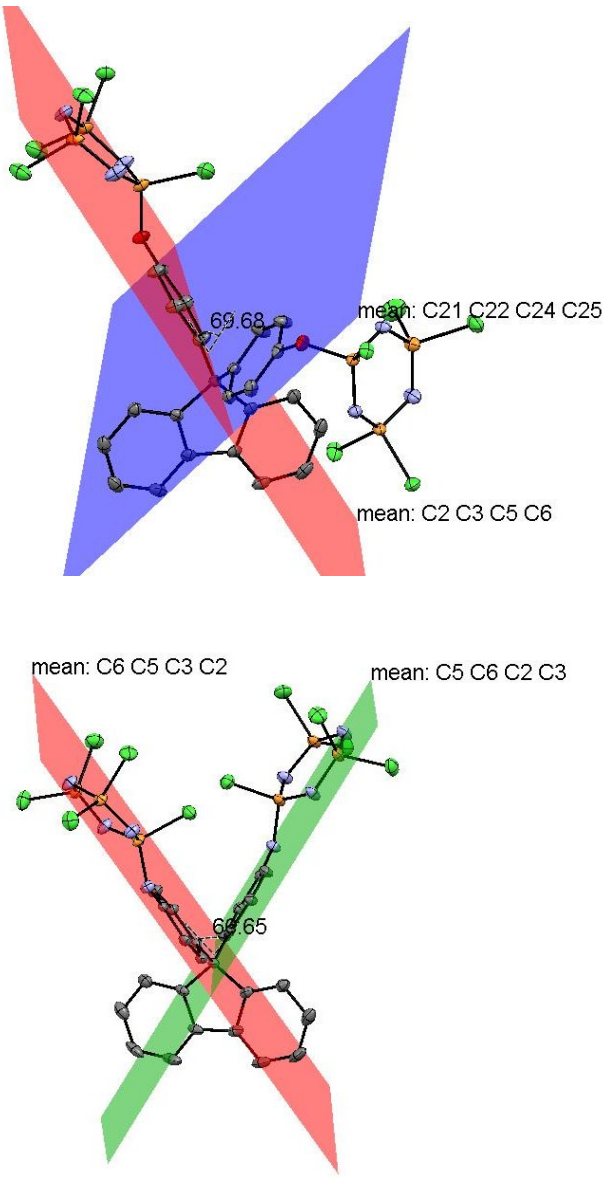

Figure S4. The angles between the planes of aniline or phenol rings of compounds **4**, and **8.**

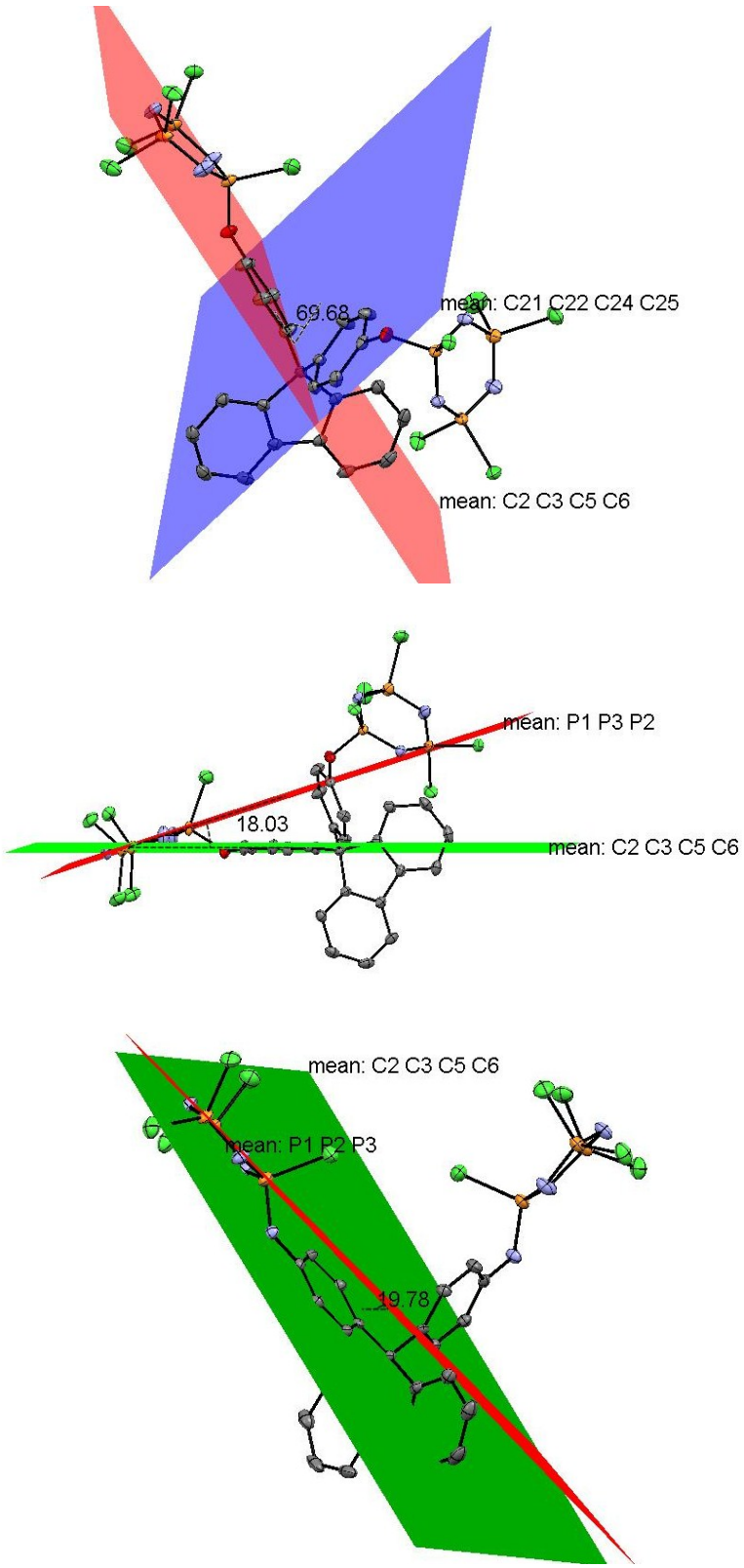

Figure S5. The angles between the planes of cyclotriphosphazene and aniline or phenol rings of compounds **4**, and **8.**

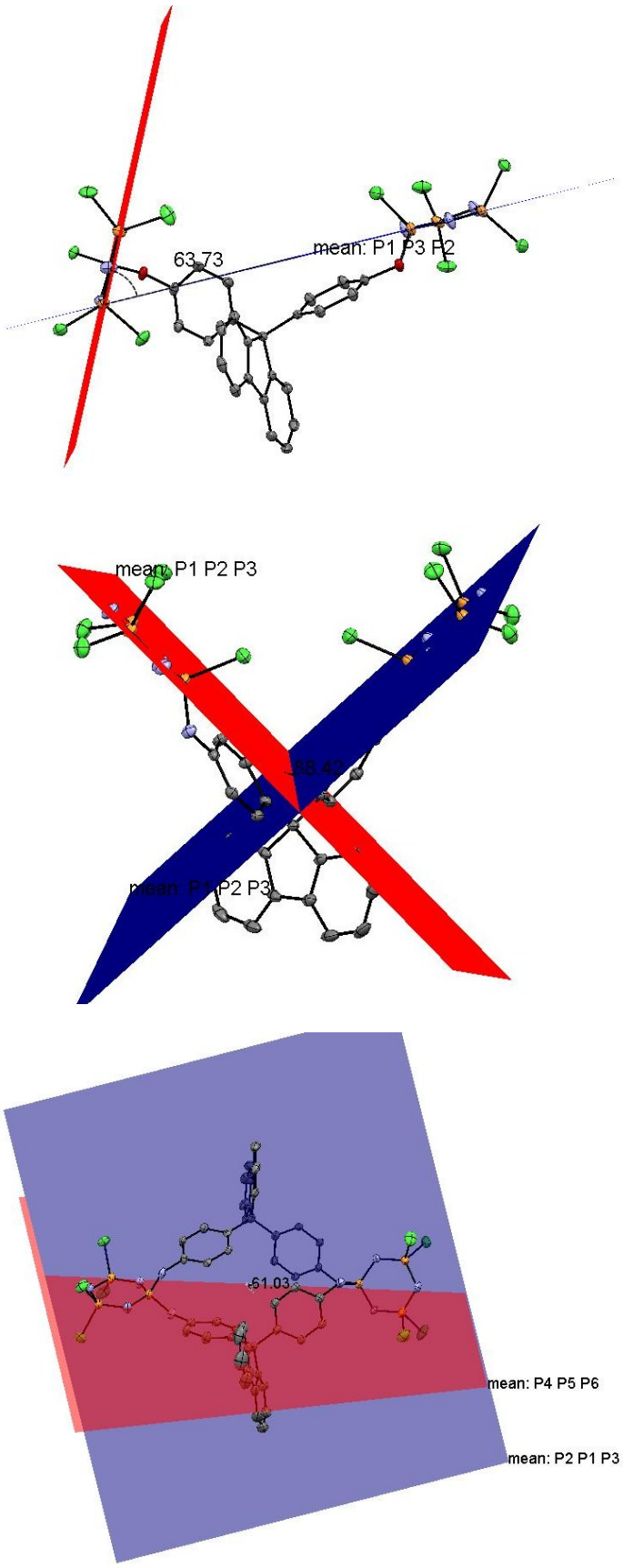

Figure S6. The angles between the planes of cyclotriphosphazene rings of compounds **4**, **8** and **9**.

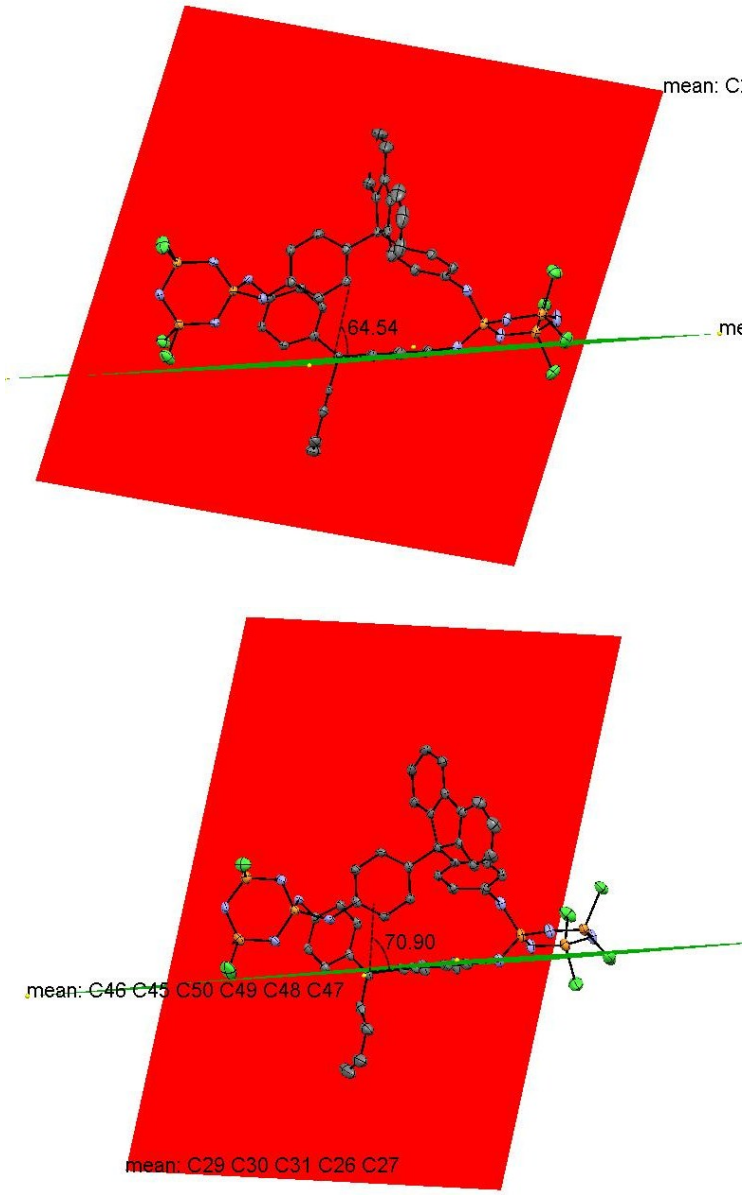

Figure S7. The angles between the planes of aniline rings of each FDA bridges of compound **9.**

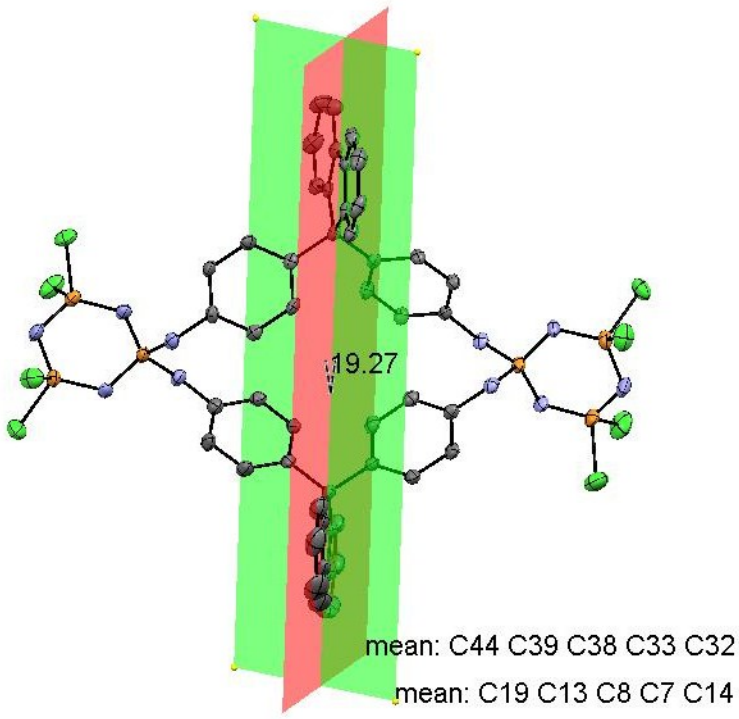

Figure S8. The angles between the planes of two fluorenylidene rings of compound **9.**

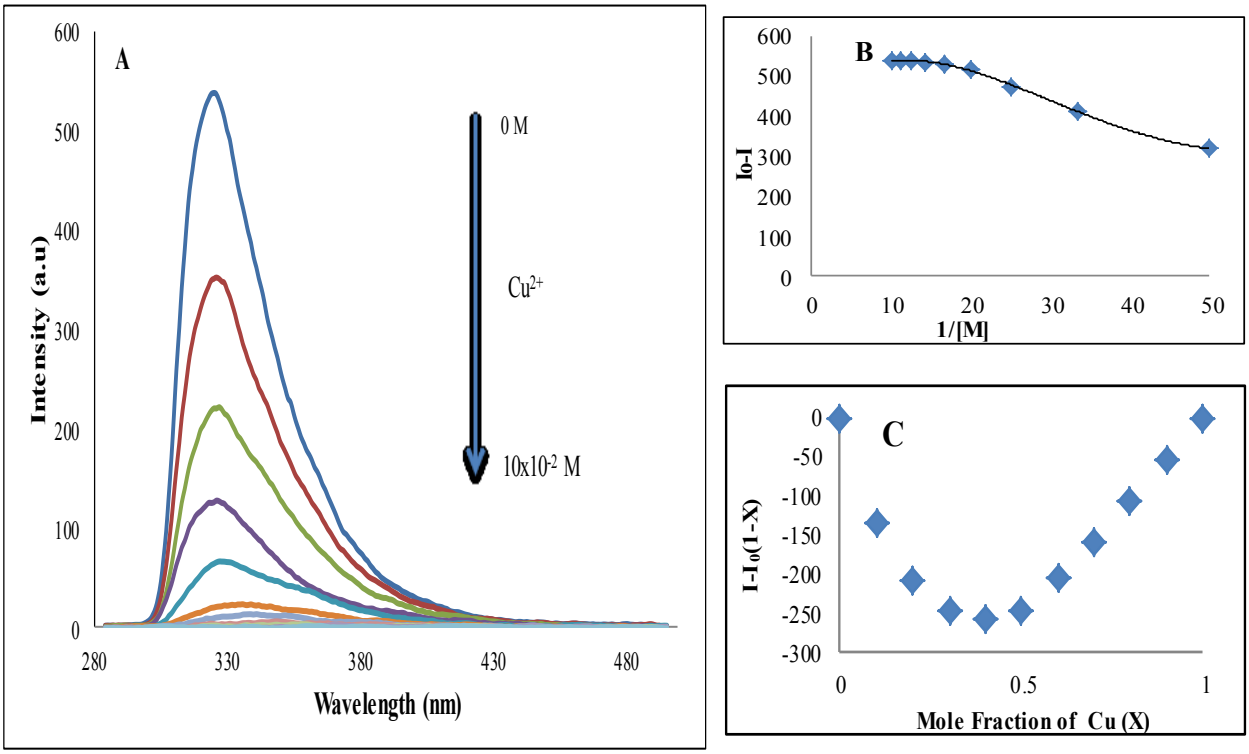

Figure S9. (A) Fluorescence response of chemosensor **3** to various equivalents of Cu^{2+}. (B) The Benesi-Hildebrand graph and (C) Job's plot of **3**-Cu^{2+} complex in THF solutions. The total concentration of **3** and Cu^{2+} was $1x10^{-2}$ M. The excitation wavelength was 270 nm. The monitored wavelength was 325 nm.

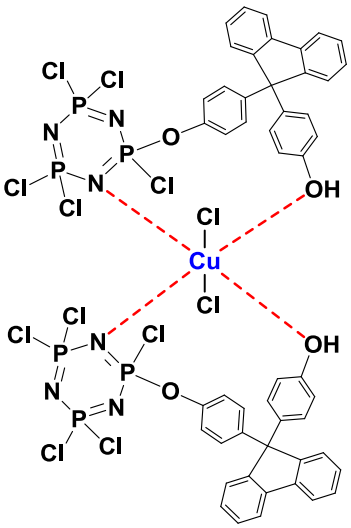

Figure S10. The proposed interaction between chemosensor **3** and Cu^{2+} ions.

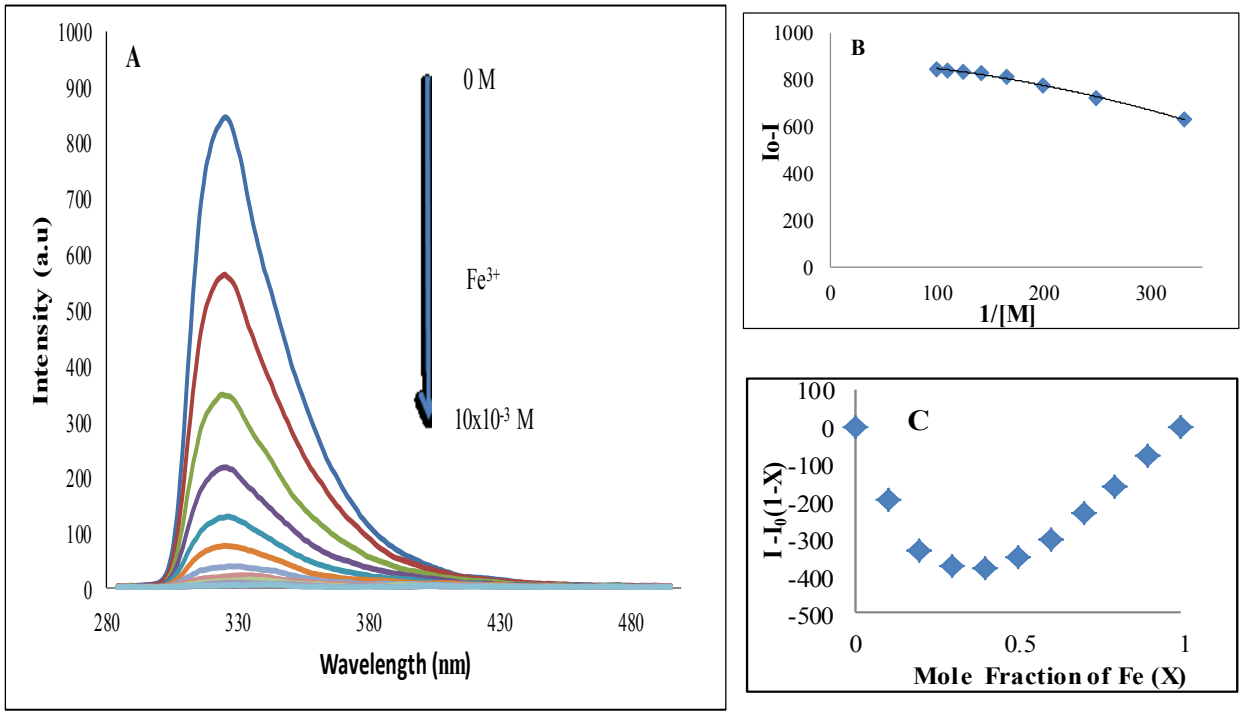

Figure S11. (A) Fluorescence response of chemosensor **3** to various equivalents of Fe^{3+}. (B) The Benesi-Hildebrand graph and (C) Job's plot of **3**-Fe^{3+} complex in THF solutions. The total concentration of **3** and Fe^{3+} was $1x10^{-3}$ M.. The excitation wavelength was 270 nm. The monitored wavelength was 325 nm.

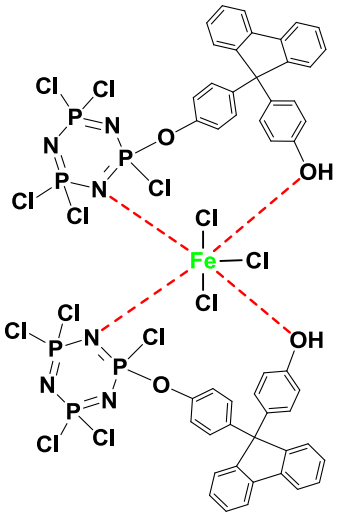

Figure S12. The proposed interaction between chemosensor **3** and Fe^{3+} ions.

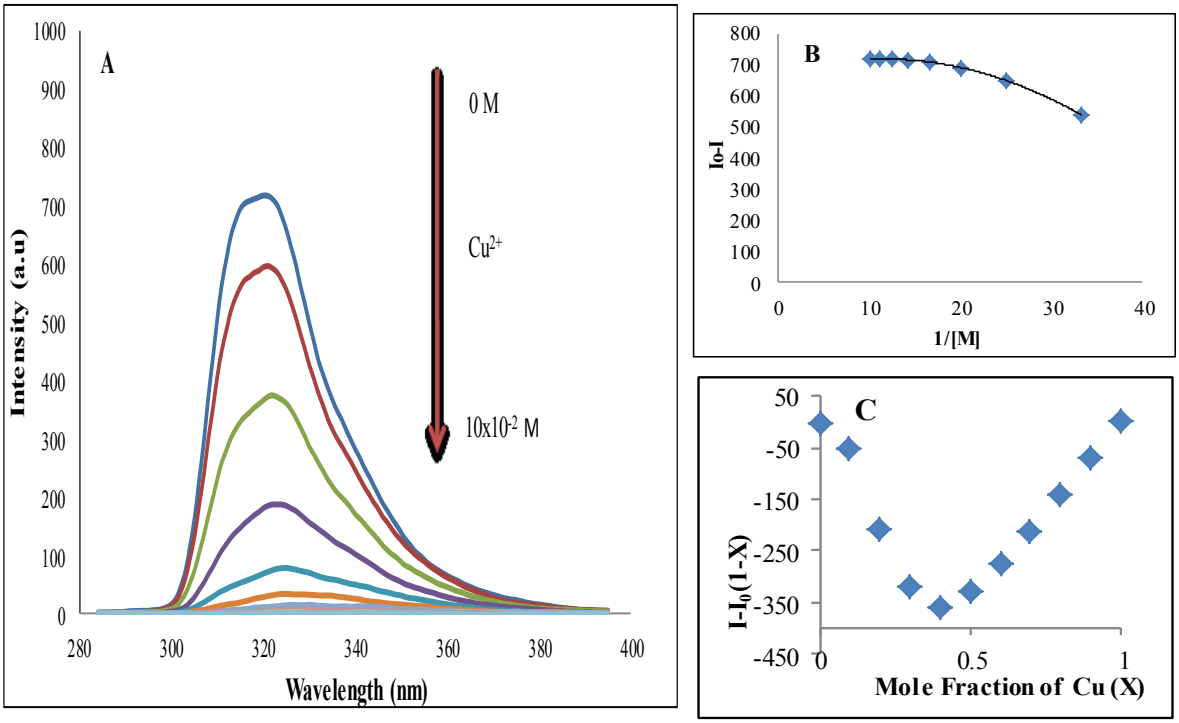

Figure S13. (A) Fluorescence response of chemosensor **4** to various equivalents of Cu^{2+}. (B) The Benesi-Hildebrand graph and (C) Job's plot of **4**-Cu^{2+} complex in THF solutions. The total concentration of **4** and Cu^{2+} was $1x10^{-2}$ M. The excitation wavelength was 270 nm. The monitored wavelength was 320 nm.

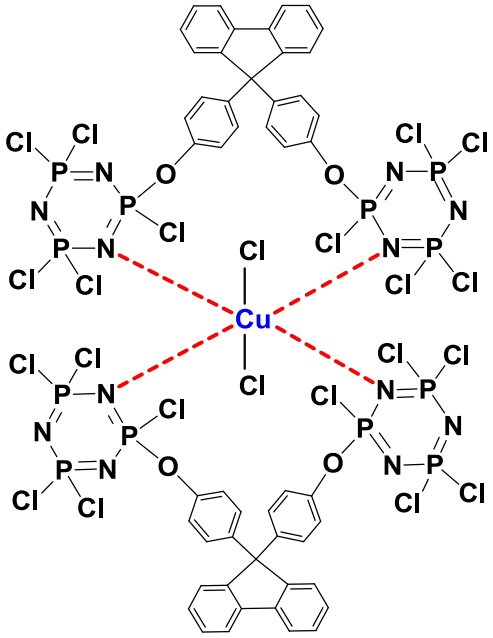

Figure S14. The proposed interaction between chemosensor **4** and Cu^{2+} ions.

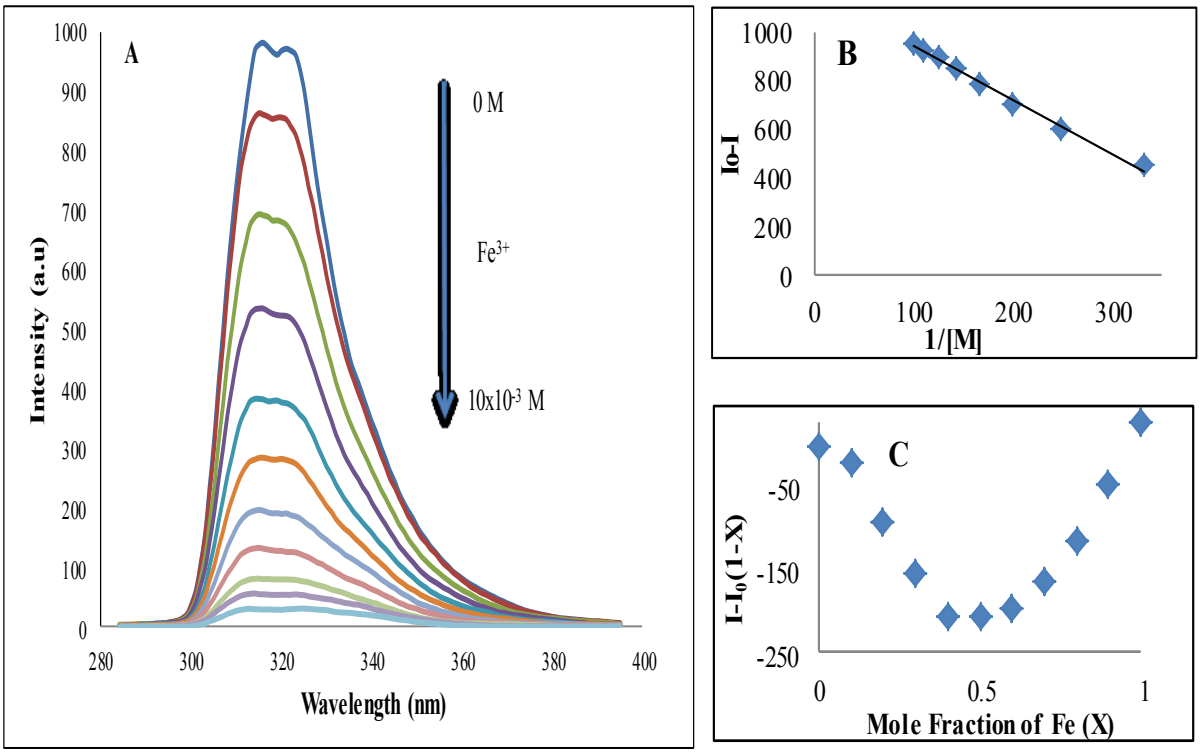

Figure S15. (A) Fluorescence response of chemosensor **4** to various equivalents of Fe^{3+}. (B) The Benesi-Hildebrand graph and (C) Job's plot of **4**- Fe^{3+} complex in THF solutions. The total concentration of **4** and Fe^{3+} was $1x10^{-3}$ M The excitation wavelength was 270 nm. The monitored wavelength was 320 nm

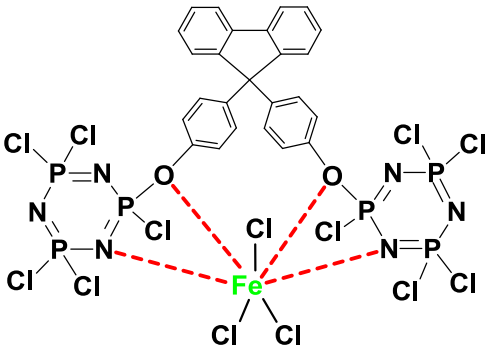

Figure S16. The proposed interaction between chemosensor **4** and Fe^{3+} ions.

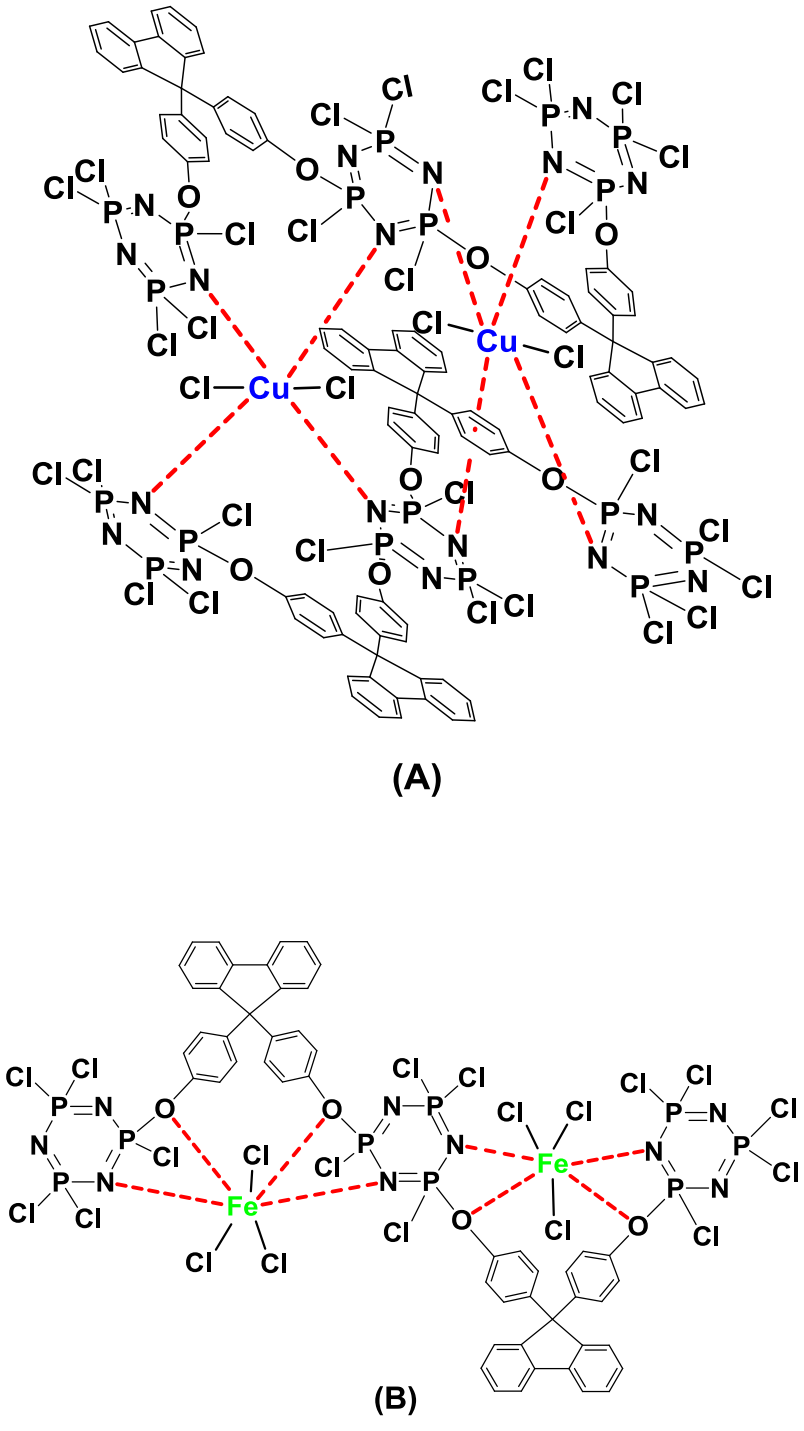

Figure S17. The proposed interaction between (A) **5** and Cu^{2+} ions and (B) **5** and Fe^{3+} ions.

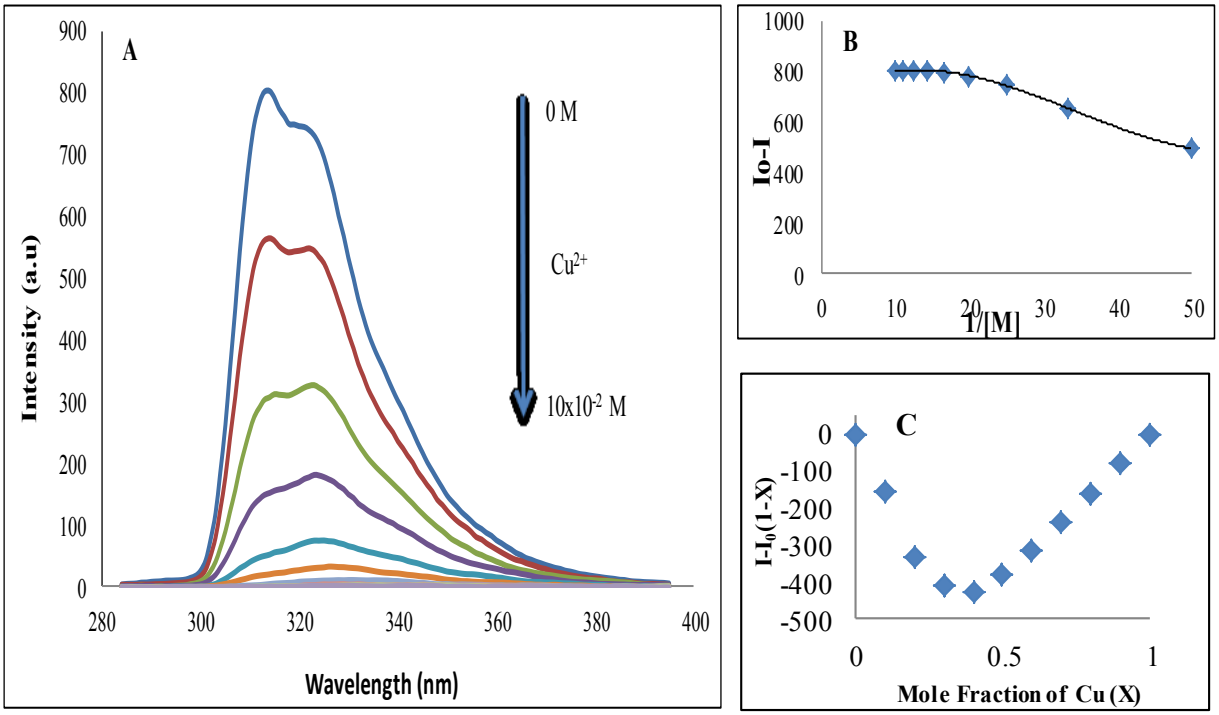

Figure S18. (A) Fluorescence response of chemosensor **6** to various equivalents of Cu^{2+}. (B) The Benesi-Hildebrand graph and (C) Job's plot of **6**-Cu^{2+} complex in THF solutions. The total concentration of **6** and Cu^{2+} was $1x10^{-2}$ M. The excitation wavelength was 270 nm. The monitored wavelength was 314 and 322 nm.

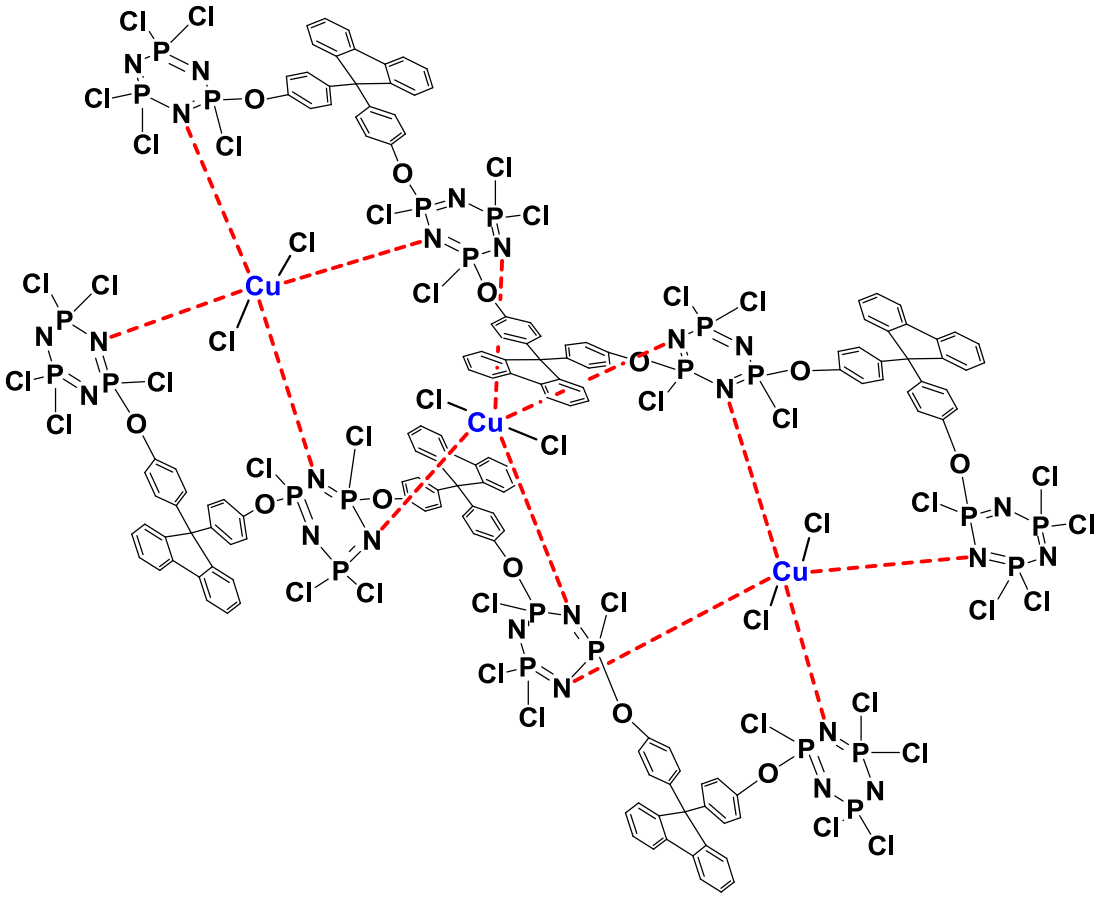

Figure S19. The proposed interaction between chemosensor **6** and Cu^{2+} ions.

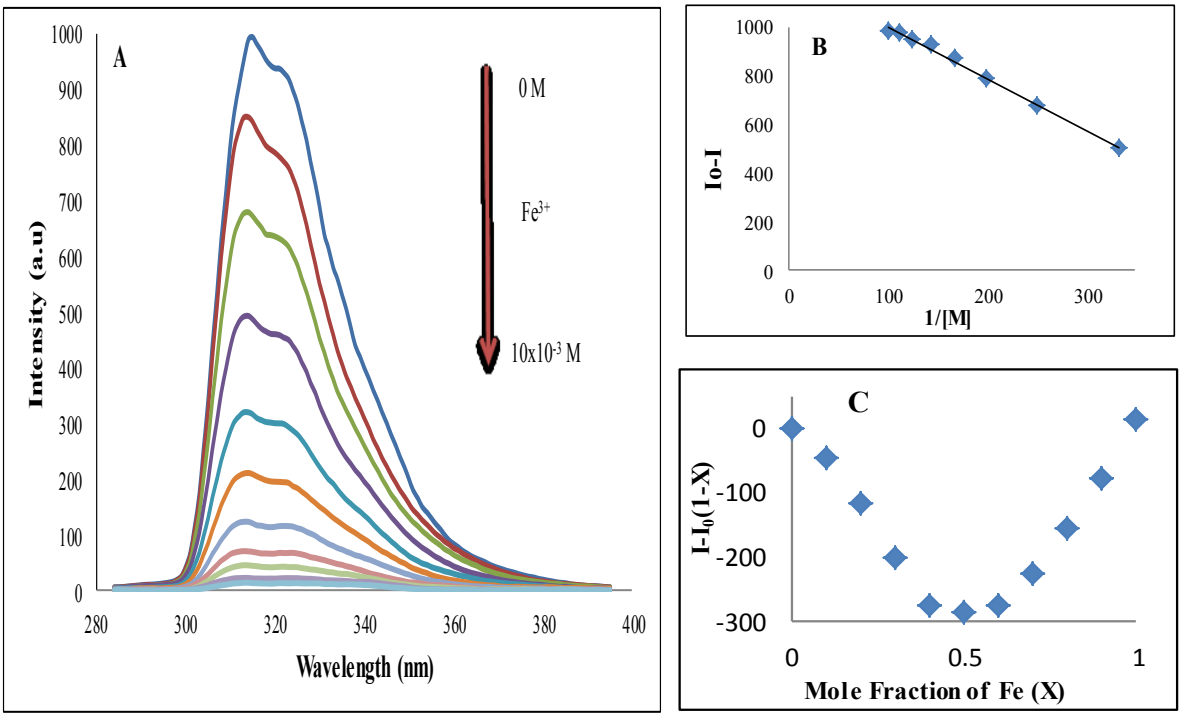

Figure S20. (A) Fluorescence response of chemosensor **6** to various equivalents of Fe^{3+}. (B) The Benesi-Hildebrand graph and (C) Job's plot of **6**- Fe^{3+} complex in THF solutions. The total concentration of **6** and Fe^{3+} was $1x10^{-3}$ M. The excitation wavelength was 270 nm. The monitored wavelength was 314 and 322 nm.

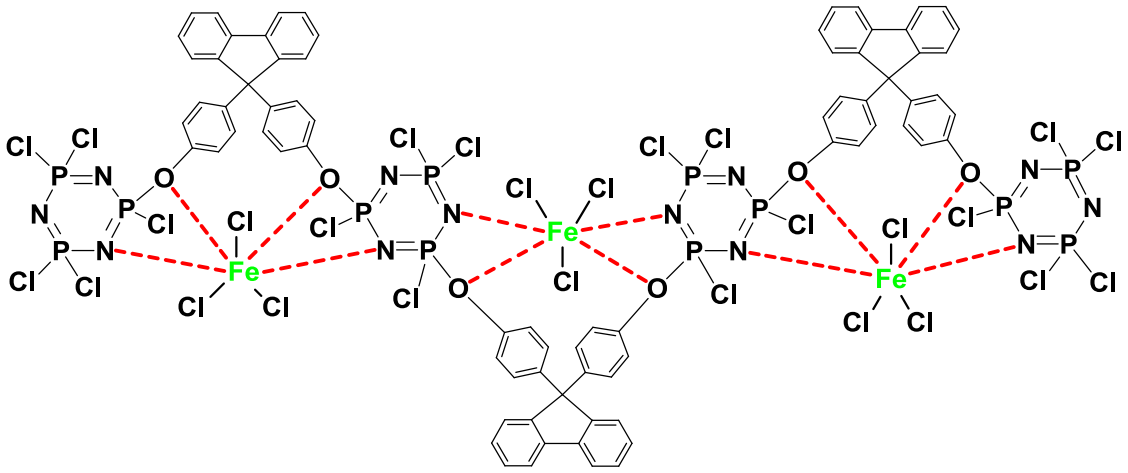

Figure S21. The proposed interaction between chemosensor **6** and Fe^{3+} ions.

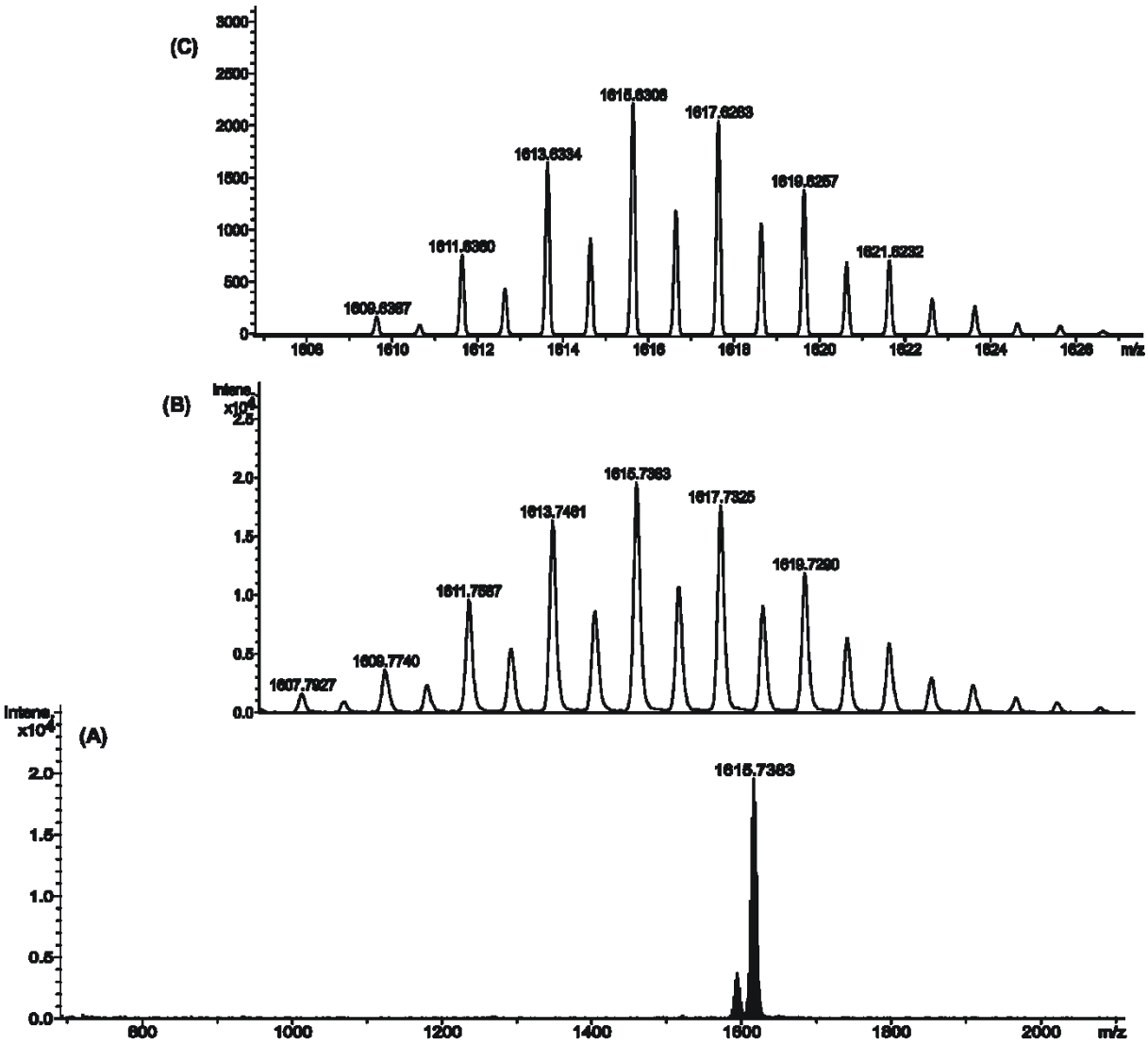

Figure S22. (A) Mass spectrum of compound **10** ESI (*m/z*)[M+Na]$^+$; (B) chloro pattern of compound **10**; (C) computer analyzing of chloro pattern of compound **10.**